9.2.3 Sampling Issues

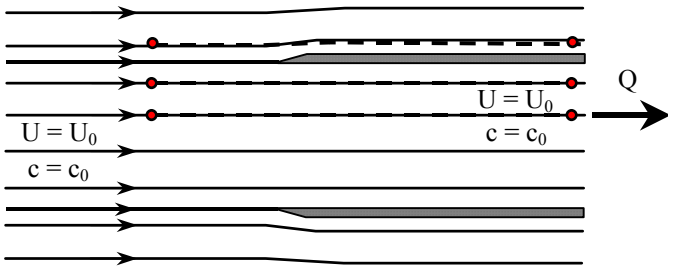

(a) isokinetic and isoaxial

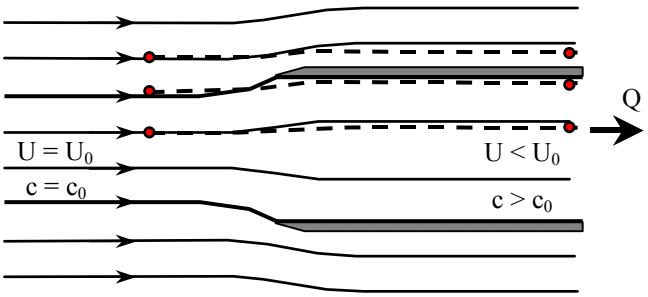

(b) subisokinetic and isoaxial

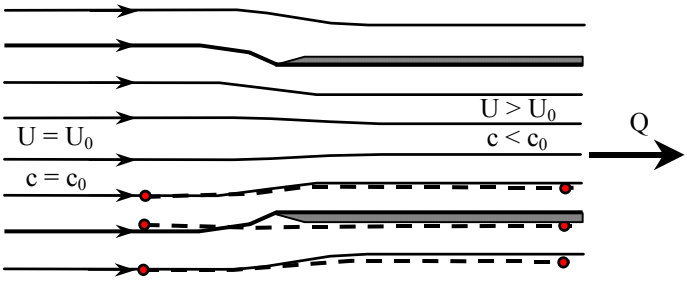

(c) superisokinetic and isoaxial

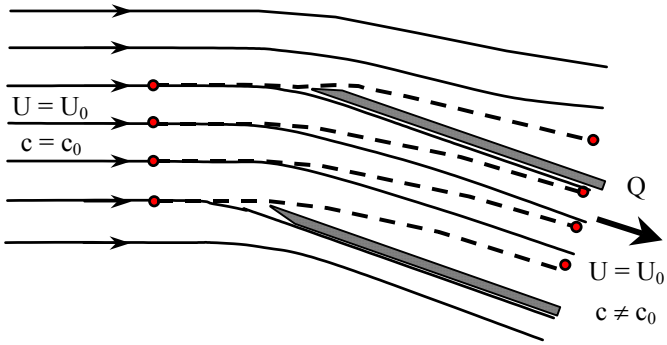

(d) isokinetic but not isoaxial

Figure 9.9 Particle trajectories (dashed) and streamlines (solid) for (a) isokinetic, isoaxial sampling, (b) subisokinetic, isoaxial sampling, (c) superisokinetic, isoaxial sampling, (d) isokinetic, but non-isoaxial sampling (misaligned sampling probe); dividing streamlines in (a), (b), and (c) are bold.

9.3 Impaction between Moving Particles

We let r_1 be the radius of particles of diameter D_p that just barely get intercepted. This defines an upstream area, πr_1^2, within which *all particles of diameter D_p or larger get collected*.

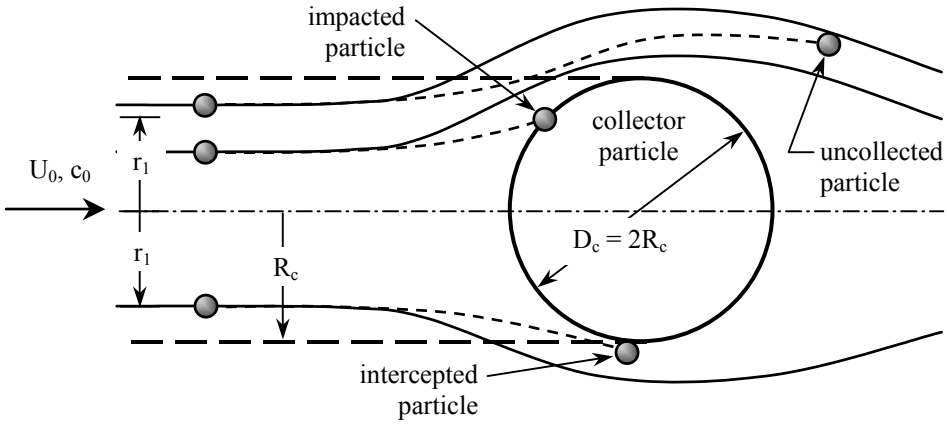

Figure 9.14 Illustration of sphere-on-sphere particle collection; solid lines are air streamlines, dashed lines are particle pathlines. Particles within radius r_1 upstream of the collecting particle impact the collecting particle, particles outside of radius r_1 pass by uncollected, and particles at radius r_1 intercept the collecting particle.

Contaminant particles initially *within* the stream tube defined by radius r_1 collide with (*impact*) the collector, while particles initially *outside* this stream tube miss the collector altogether, even for cases in which $r_1 < R_c$, as shown in Figure 9.14. For the limiting case of particles initially *at* radius r_1, their surfaces just barely collide with (*intercept*) the collector, as also sketched. Not shown in Figure 9.14 is the removal of very small particles that diffuse to the surface of the collector. ***The single drop, sphere-on-sphere removal efficiency*** (η_d) is defined as the fraction of particles in the stream tube defined by the collector that are removed by the processes of impaction, interception, and diffusion:

$$\eta_d = \frac{c_0 \pi r_1^2 U_0}{c_0 \pi R_c^2 U_0} = \left(\frac{r_1}{R_c} \right)^2 \tag{9-12}$$

Similar expressions can be defined for impaction of spheres on cylinders or for any pair of impacting bodies.

9.3.1 Single Drop Collection Efficiency

The single drop collection efficiency (η_d) of spheres impacting on spheres may be written as a function of Stokes number (Stk), as defined in Chapter 8:

$$\mathrm{Stk} = \frac{\tau_p \left| \vec{v}_r \right|}{D_c} \tag{9-13}$$

where τ_p is the relaxation time constant for the particle, also defined in Chapter 8 as

$$\tau_p = \frac{\rho_p D_p^2}{18\mu} \tag{9-14}$$

and $\vec{v}_r$ is the velocity of the particle relative to the collector,

$$\vec{v}_r = \vec{v}_p - \vec{v}_c \tag{9-15}$$

where $\vec{v}_p$ is the velocity of the particle and $\vec{v}_c$ is the velocity of the collector. If gravimetric settling is neglected, the particle travels at a velocity equal to the gas velocity, $\vec{v}_p = \vec{U}_o$. A graph of the single drop

collection efficiency for spheres impacting on spheres shows that η_d is zero at Stokes number Stk = 0.083, and asymptotically approaches unity for large values of Stk. Calvert and Englund (1984) recommend that for flows in which the Stokes number exceeds 0.2, the single drop collection efficiency of spheres impacting on spheres can be approximated by

$$\eta_d = \left(\frac{\text{Stk}}{\text{Stk} + 0.7} \right)^2 \qquad \text{for Stk} > 0.2 \tag{9-16}$$

Example 9.2 – Single Drop Collection Efficiency of Rain Drops falling through Dusty Air

Given: Consider rain drops with a diameter range of 5 μm ≤ D_c ≤ 500 μm, falling through air containing dust particles with a diameter range of 5 μm ≤ D_p ≤ 50 μm.

To do: Compute and plot the single drop collection efficiency (η_d) as a function of D_c and D_p.

Solution: Equation (9-16) predicts the single drop collection efficiency (η_d) as a function of Stokes number. Since the dust particle is motionless, the relative velocity is equal to the terminal settling velocity of the rain drop (v_c) which in turn varies with its diameter (D_c), as discussed in Chapter 8. The particle relaxation time (τ_p) is a function of dust particle diameter (D_p), as given by Eq. (9-14). To compute the efficiency, the drop's terminal settling velocity (v_c) is calculated for a particular value of D_c, and then the efficiency for various values of D_p is calculated. The process is repeated for various combinations of D_c and D_p, recognizing that the drag coefficient c_D is a function of Reynolds number, which complicates the calculations. The authors used Mathcad to accomplish this task. Figure E9.2 shows the single drop collection efficiency of a raindrop falling through dusty air.

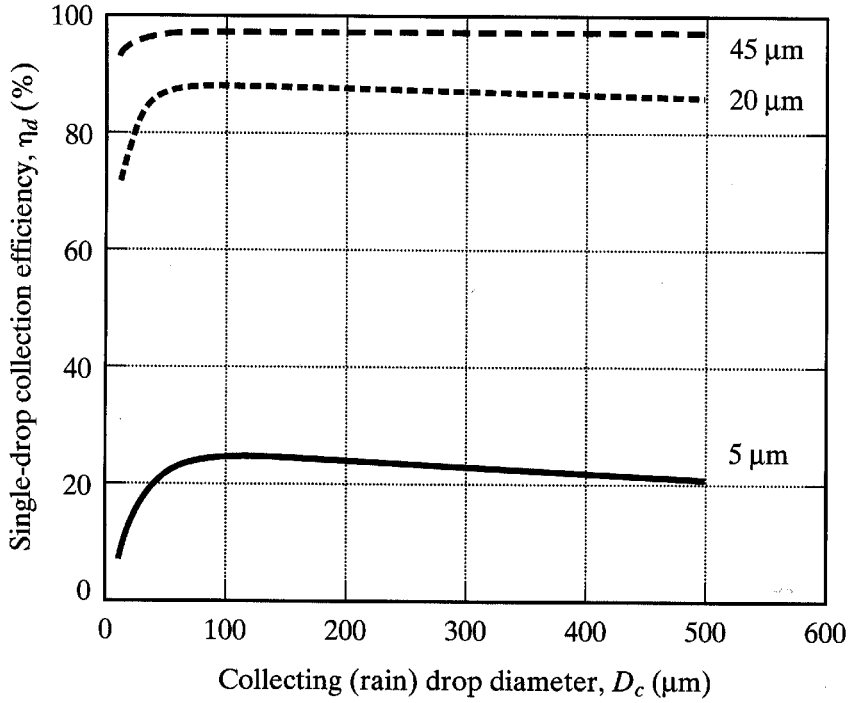

Figure E9.2 Ability of rain to remove airborne dust. Single drop collection efficiency of various size rain drops (μm) falling freely through still air containing dust particles, D_p = 5, 20, and 45 μm, ρ_p = 1,000 kg/m^3 (from Heinsohn & Kabel, 1999).

Discussion: Readers may be surprised to see the efficiency reach a maximum and then fall for large drop diameters. The explanation turns on how settling velocity varies with drop diameter. For small drop diameters, the Reynolds number is small, Stokes flow exists, and the settling velocity increases with the square of drop diameter. Thus Stokes number increases linearly with D_c and the efficiency rises with D_c. For large values of D_c, the Reynolds number is large and the drag coefficient approaches a constant (0.4). Thus, settling velocity increases with the *square root* of D_c, and Stokes number is inversely proportional to the square root of D_c. As D_c increases, Stokes number therefore falls and the efficiency falls as well. The results shown in Figure E9.2 should be checked to ensure that Stokes number (Stk) is greater than 0.2 for each case.

9.3.2 Spray Chambers *(Engineers create "artificial rain" to remove particles from air)*

The overall effectiveness of a ***counterflow spray chamber***, as in Figure 9.15, can be modeled using an approach suggested by Calvert (1972) and Crawford (1976). The following assumptions are made:

- The height of the control region is L. The diameter of the collecting drops (D_c) and the absolute velocity ($\vec{v}_c$) of the falling drops are constants.
- The diameter of the contaminant particles (D_p) is constant and the number concentration of contaminant particles (c_{number}), varies only with height (z).
- The number concentration of collecting drops ($c_{number,c}$) is uniform; the number of encounters between particles and collecting drops (n) is uniform.
- The volumetric flow rates of air (Q_a) and spray liquid (Q_s) are constants.
- Gravimetric settling of the small contaminant particles is negligible; it is assumed that the velocity of these particles ($\vec{v}_p$) is equal to the air velocity ($\vec{U}_a$) which is constant,

$$\boxed{\vec{v}_p = \vec{U}_a} \qquad (9\text{-}17)$$

- The velocity of impaction is the velocity of the particle relative to that of the collector,

$$\boxed{\vec{v}_{impaction} = \vec{v}_p - \vec{v}_c = \vec{U}_a - \vec{v}_c} \qquad (9\text{-}18)$$

Because the air and particles flow upward and the drops fall downward, the impaction speed is the sum of the air speed and the drop speed, which in turn is equal to the magnitude of the settling velocity ($v_{t,c}$) of the collector particle in quiescent air:

$$\boxed{v_{t,c} = U_a + v_c} \qquad (9\text{-}19)$$

The number of collecting drops per unit volume of air ($c_{number,c}$) can be calculated from the mass flow rate of the scrubbing liquid ($\dot{m}_c$), which is a parameter controlled by the engineer; $\dot{m}_c$ can be expressed by

$$\boxed{\dot{m}_c = \overline{\rho}_c v_c A} \qquad (9\text{-}20)$$

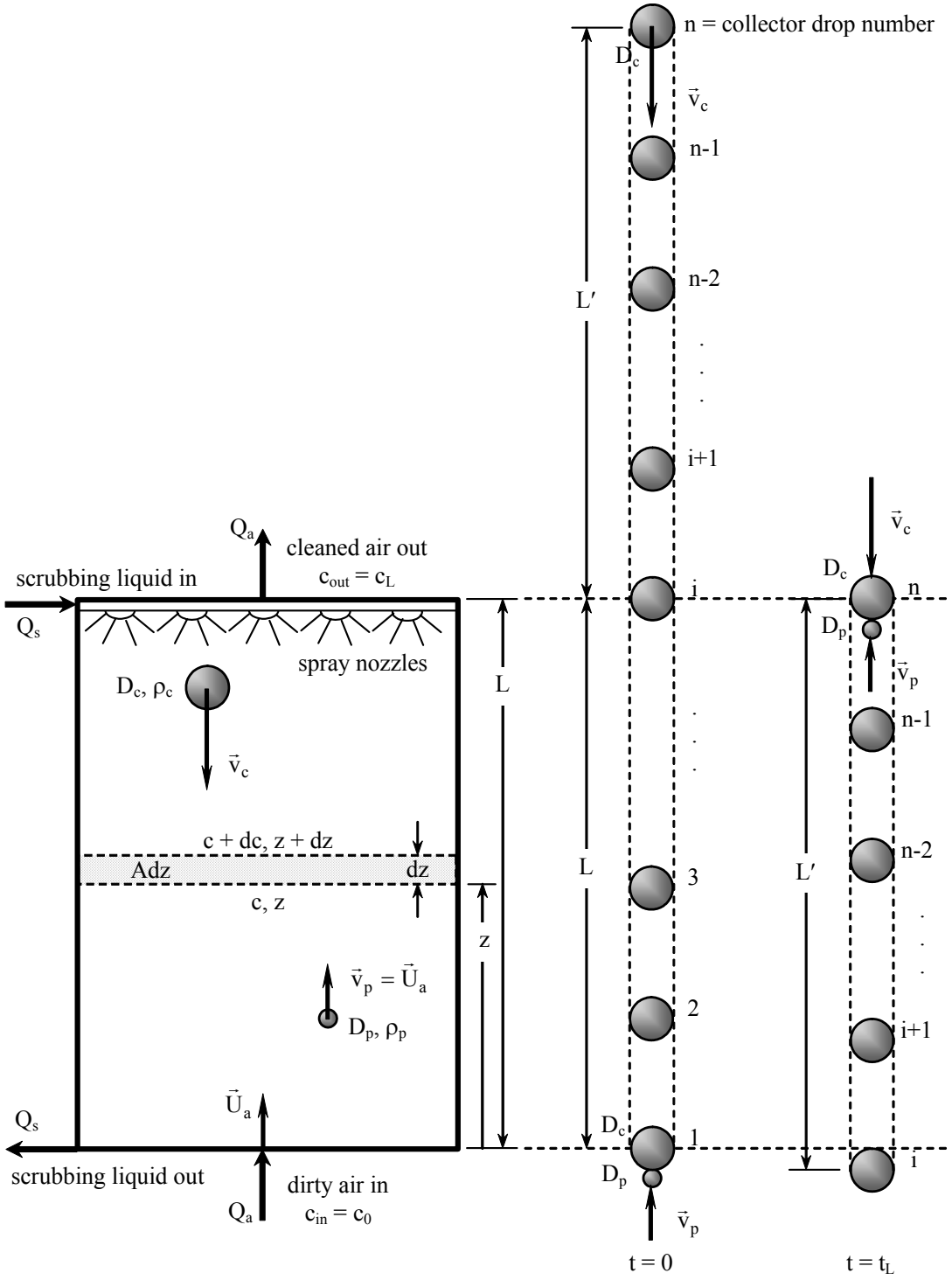

Figure 9.15 Schematic diagram of a vertical counterflow spray chamber illustrating encounters between upward traveling contaminant particles and falling collector drops; at t = 0, contaminant particles at the bottom of the chamber encounter drop 1, and at t = t_L, contaminant particles at the top of the chamber encounter drop n.

Each drop acts like a particle collector *in series* with the other drops. Thus, the grade efficiency for the column for particles of diameter D_p can be constructed as follows:

$$\eta\left(D_p\right) = 1 - \frac{c_{out}\left(D_p\right)}{c_{in}\left(D_p\right)} = 1 - \left(\frac{c_{out}}{c_{n-1}}\right)\left(\frac{c_{n-1}}{c_{n-2}}\right)\ldots\left(\frac{c_3}{c_2}\right)\left(\frac{c_2}{c_1}\right)\left(\frac{c_1}{c_{in}}\right)$$

After some algebra – see the text, one obtains the following expression for the grade efficiency of a vertical, counter-flow spray chamber:

$$\boxed{\eta\left(D_p\right) = 1 - \frac{c_{out}\left(D_p\right)}{c_{in}\left(D_p\right)} = 1 - \exp\left[-\frac{3}{2}\eta_d \frac{v_{t,c}}{v_c}\frac{Q_s}{Q_a}\frac{L}{D_c}\right]} \qquad (9\text{-}30)$$

9.3.3 Transverse Packed Bed Scrubbers

An alternative design is the ***transverse packed bed scrubber*** shown schematically in Figure 9.16.

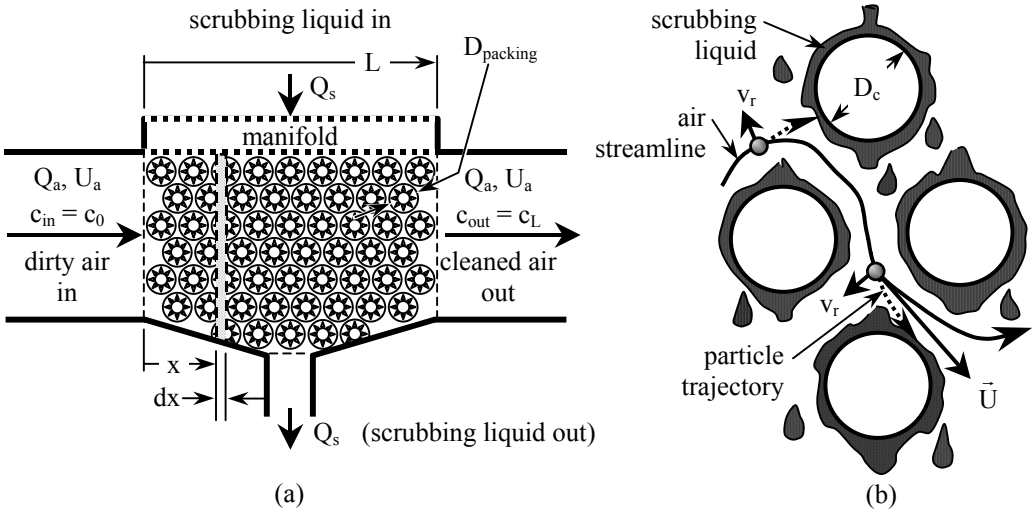

Figure 9.16 Transverse packed bed scrubber: (a) overall schematic diagram; (b) magnified view of curvilinear air flow through packed bed, generating radial particle velocities (v_r) that cause particles to impact wetted packing material of characteristic diameter D_c.

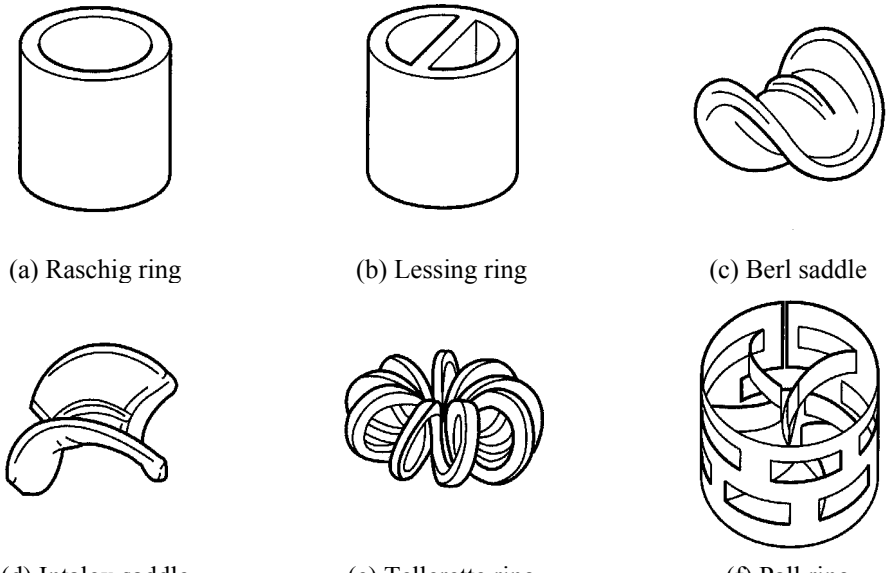

Figure 9.17 Packing elements of various sizes, shapes, and materials, depending on application.

See algebra in the text – we get a similar expression for the grade efficiency for the removal efficiency for particles of diameter D_p, i.e.,

$$\eta(D_p) = 1 - \frac{c_L}{c_0} = 1 - \exp\left[-2C\frac{\tau_p a_p U_a}{D_c \varepsilon^2} L\right]$$

or

$$\eta(D_p) = 1 - \exp\left[-2C\left(Stk\right)\frac{a_p}{\varepsilon^2}L\right] \tag{9-35}$$

where Stokes number (Stk) is defined as

$$Stk = \frac{\tau_p U_a}{D_c} = \frac{\tau_p Q_a}{D_c A_{bed}} \tag{9-36}$$

9.4 - Filtration

Filtration is the name given to the removal of particles as they pass through some permeable material such as paper, felt, or woven cloth, or through a bed of collectors. See Billings and Wilder (1970) for a more detailed discussion of filtration. Filtration is the most common method of collecting particles, and applications are found in general HVAC air cleaners, specialized laboratory air cleaners (e.g. clean rooms), and in health care equipment and facilities. Filtration units are often part of large air pollution control systems such as are those used to collect particles discharged by electric utility boilers, kilns, etc.; volumetric flow rates can reach hundreds of thousands of CFM. Filtration units may also be small uncomplicated units that capture particles generated by individual machines inside a plant, e.g. downdraft grinding benches, grinding wheels, wood sanding machines, etc. It is often more economical to capture particles by a small filter mounted to a machine rather than to install ducts connecting the machine to a large central air cleaning system for the entire plant.

9.4.1 Baghouses

Baghouse is the name given to a large filtration system containing many fabric filter bags arranged in modules operating in parallel. There are three principal types of baghouse, each using a different method to remove the collected dust from filters:

- shaker fabric baghouse
- reverse-flow baghouse
- pulse-jet baghouse

Shaker Fabric Baghouse: Figure 9.23 shows a schematic diagram of one module of a ***shaker fabric baghouse***. Individual cylindrical filters in the baghouse are approximately 10 inches in diameter and 10-15 ft long, and are held taught by hangers attached to the top of the closed bag. The bags are packed closely with only a few inches separating one from another. Dozens of bags are contained in a module, and a baghouse consists of many modules arranged in parallel to receive the dust laden process gas stream. The bottom of each bag is clamped to a ***tube sheet***, which has openings for each bag as illustrated in Figure 9.23. Dust laden air enters the bottom of the module, passes through the tube sheet, and into the inside of the filter bags. As the dirty air travels upward, clean air can pass through the bags, but most of the particles are trapped inside and deposited on the inside surfaces of the bags. A ***dust cake*** therefore accumulates on the inside of each bag. Once formed, the dust cake functions as a filter. In a sense, the woven fabric is merely the substrate to hold the dust cake – it is the dust cake that performs the bulk of the collection. Cleaned air passes through the outside of the bag into a plenum that receives cleaned air from other modules. Cleaned air finally leaves the module through an outlet duct. Periodically an entire module is taken off-line; it is isolated by damper valves, and its individual filters are cleaned by shaking them at the top. The dust cake on the inside of the bag fractures and falls below to the hopper. The module is allowed to rest for a few minutes until the dust settles, and the cleaned module is placed back on-line. Note that the dust cake is assumed to be ***friable***, which means that it easily crumbles to powder; otherwise it may not dislodge from the bag.

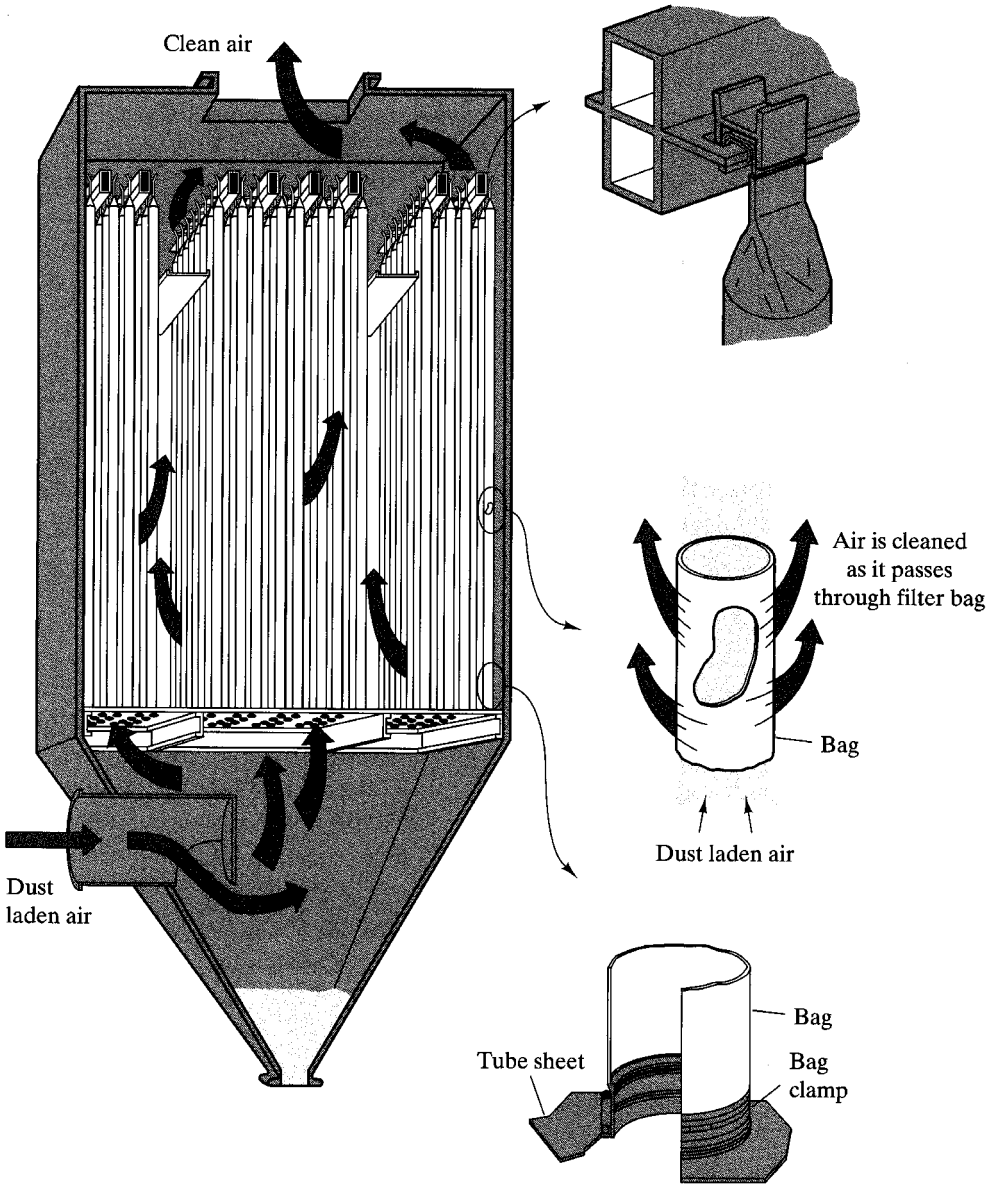

Figure 9.23 One module of a shaker fabric baghouse; bag closed with shaker at the top, open and sealed at the bottom; there are 128 bags in this module.

Reverse-Flow Baghouse: Figure 9.24 shows a schematic diagram of one module of a ***reverse-flow baghouse***. The fundamental features of a reverse-flow baghouse are the same as those of a shaker baghouse, except instead of shaking the bags to remove the dust cake, reverse air flow is used. A pulse of cleaned air is forced into the module from the top. This reverse-flow air compresses portions of each filter bag, as illustrated in Figure 9.24, whereupon the dust cake is dislodged and falls to the hopper below. Meritt and Vann Bush (1997) report that low-frequency sonic horns are installed in approximately 80% of the reverse-flow baghouses used for coal-fired utility boilers (excluding those using dry flue gas desulfurization). Sonic energy augments the fabric movement caused by reverse flow and dislodges additional dust cake material from the fabric.

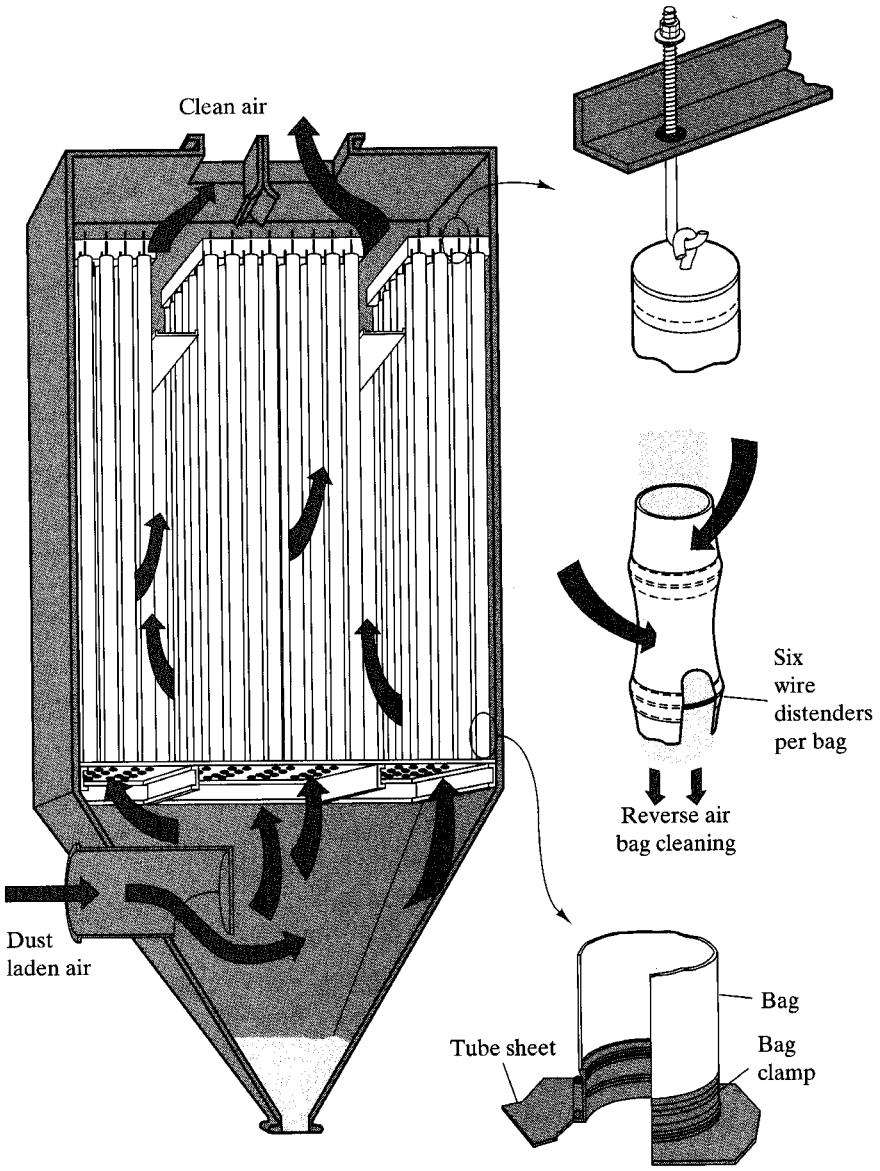

Figure 9.24 One module of a reverse-flow baghouse; bag closed and hung from the top, open and sealed at the bottom; there are 112 bags in this module.

Pulse-Jet Baghouse: The fundamental difference between a shaker or reverse-flow baghouse and a pulse-jet baghouse is that dust laden air passes radially *inward* into the bag in a pulse-jet baghouse, but flows radially *outward* through the bag in shaker and reverse-flow baghouses. Thus dust accumulates on the *outside* surface of the pulse-jet bag and on the *inside* surface of shaker and reverse-flow bags. A schematic diagram of a ***pulse-jet baghouse*** is shown in Figure 9.25. A pulse-jet baghouse contains cylindrical fiber filters surrounding cylindrical wire cages that maintain the cylindrical shape and allow air to flow radially inward through the filters. The filter bags are closed at the bottom but open at the top, where they are clamped to a tube sheet. Dust laden air enters the plenum surrounding the bags; cleaned air passes inward through the bag and

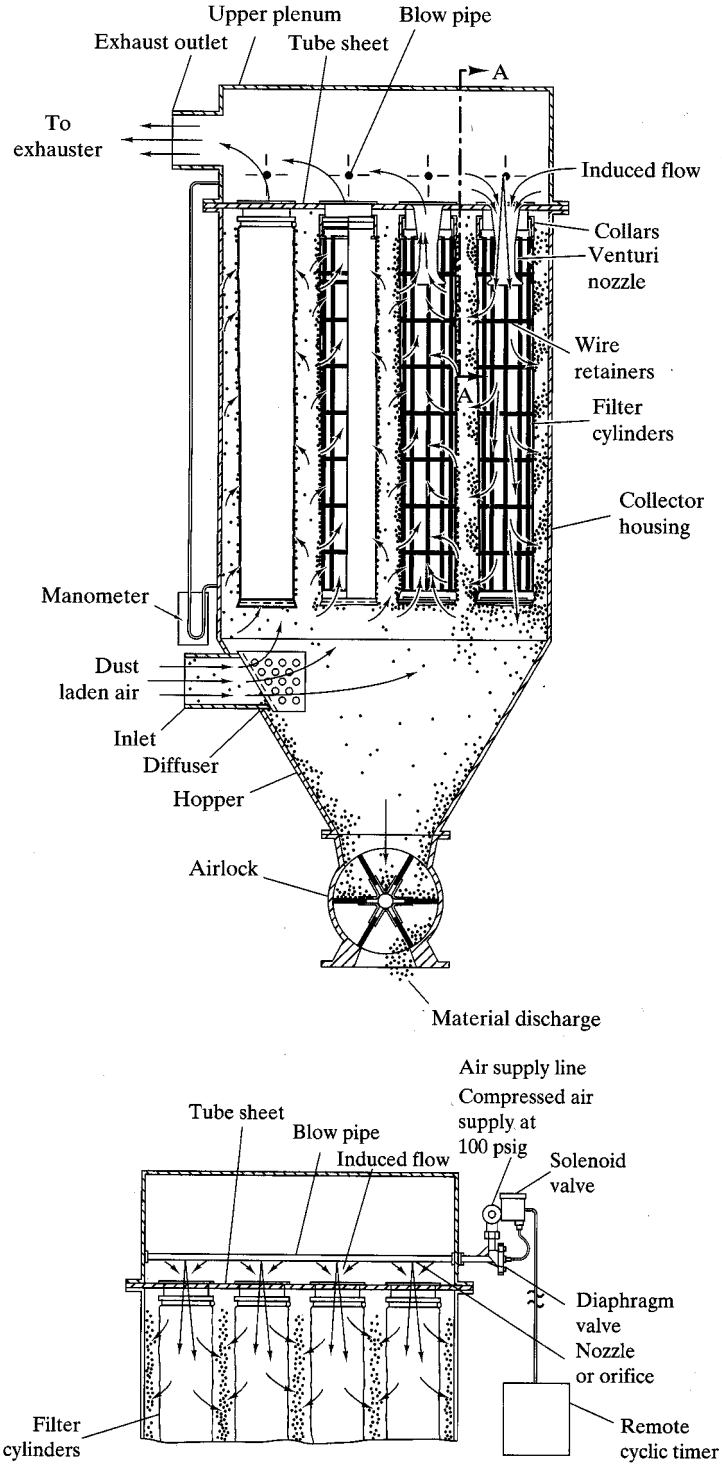

Figure 9.25 Pulse-jet baghouse; cutaway view at top shows internal wire cage; bag open and sealed at the top, closed at the bottom; there are 16 bags in this module.

exits the top of the bag, while dust builds up on the outside surface of the bag. Periodically a high-pressure pulse of air passes through nozzles at the top of each filter bag. The air pulse travels downward, flexes the bag outward, and dislodges dust collected on the outside of the filter; the dust then falls into the hopper below.

Following cleaning, the high-pressure air jet ceases, dust-laden gas again tries to enter the bag, and dust is once again collected on its exterior surface.

Two major features differentiate pulse-jet filters from reverse-flow and shaker filters:

(a) Reverse-flow and shaker filters are cleaned every one-half to several hours. Pulse-jet filters are cleaned every few minutes. Thus the weight of the collected dust (dust cake) can become large for reverse-flow and shaker filters but is very small for pulse-jet filters. The dust cake from a reverse-flow baghouse weighed 40-60 lbf/bag, as measured by Carr and Smith (1984), who also report that only about 10% of the dust is removed per cleaning cycle, implying that much of the dust is trapped within the filter fibers, as illustrated in Figure 9.26.

(b) Pulse-jet filters are composed of ***felt*** material whereas shaker and reverse-flow filters are composed of woven fabric. Woven fabrics are constructed of yarn woven to provide the tensile strength needed by the fabric to withstand the large dead weight of the dust cake and flexure properties needed to withstand the cleaning process. Felts consist of fibers that adhere to one another because of adhesive applied to the surface of each fiber. Felts do not have the tensile strength of woven fabrics, so felt filters surround a cylindrical wire structure to maintain its cylindrical shape. Figure 9.27 shows the fundamental differences between woven fabric and felt.

Filter collectors may be woven fibers as seen in Figure 9.27a and 9.27b, or a bed of tightly packed matted fibers (felt), as in Figure 9.27c. Alternatively, the bed may consist of a layer of individual collected particles attached to the filter fabric through which the aerosol passes, as in Figure 9.26. Particles are removed as they impact on the collectors. Industrial filters often combine both phenomena since the dust cake on the upstream (dirty) side of a filter acts as a filter bed while the filter fabric itself removes additional particles and supports the dust cake.

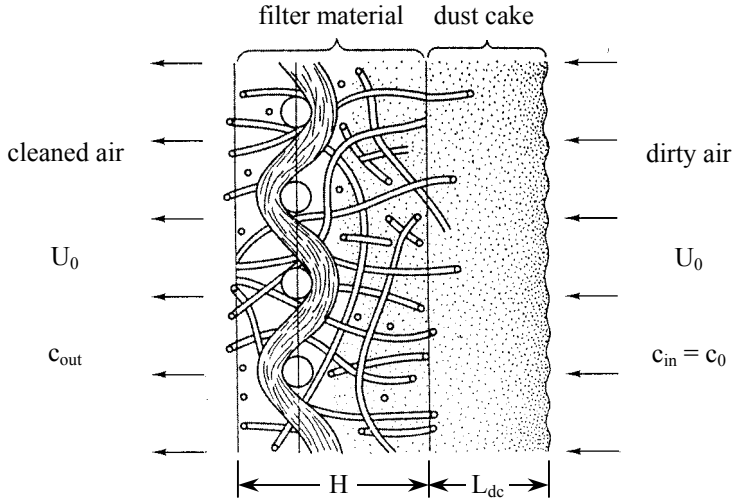

Figure 9.26 Schematic diagram of filter material of thickness H and dust cake of thickness L_{dc}, which varies with time.

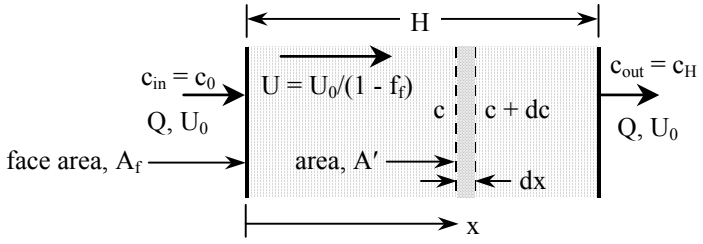

Figure 9.31 Schematic diagram illustrating an analytical model of flow through a filter.

To model the overall collection efficiency, it is necessary to define the following parameters:

- fiber solids fraction (f_f)
- length of fiber per unit volume of filter (L_f)

The ***porosity*** (ε) of the filter is defined as the fraction of the overall filter volume that is open. The porosity is also called the ***voidage*** or ***void fraction***. The ***fiber packing density*** (f_f), also called the ***fiber solids fraction***, is the fraction of the overall filter volume that is composed of solids (fibers). f_f is related to the porosity by

$$\boxed{f_f = 1 - \text{porosity} = 1 - \varepsilon} \tag{9-55}$$

By similar reasoning, f_f is the ratio of the bulk density of the filter to the density of the fiber material, as per Eq. (9-39). Similarly, f_f is equal to the ***blockage***, the fraction of the cross-sectional area of the filter that is composed of solid matter,

$$\boxed{f_f = 1 - \frac{A'}{A_f}} \tag{9-56}$$

where A' is the cross-sectional area through which air actually moves inside the filter. The speed of the aerosol inside the filter (U) is related to the approach speed (U_0) by

$$\boxed{U = \frac{U_0 A_f}{A'} = \frac{U_0}{1 - f_f} = \frac{U_0}{\varepsilon}} \tag{9-57}$$

The ***length of fiber per unit volume of filter*** (L_f) is defined as follows. For simplicity, imagine that the filter is composed of a single fiber of length L_{fiber} and of diameter D_f convoluted like a long spaghetti noodle into filter volume V defined by the outer boundaries of the filter. The fiber solids fraction (f_f) can then be written as the ratio of fiber volume to total filter volume,

$$f_f = \frac{\frac{\pi}{4} D_f^{\,2} L_{fiber}}{V}$$

In terms of fiber solids fraction and fiber diameter, L_f can thus be written as

$$\boxed{L_f = \frac{L_{fiber}}{V} = \frac{4 f_f}{\pi D_f^{\,2}}} \tag{9-58}$$

Consider air carrying contaminant particles as it passes through the filter. A mass balance for the contaminant in the elemental filter volume shown in Figure 9.31 can be written as a first-order ODE, which can be integrated to yield the grade efficiency, $\eta(D_p)$, of the filter for particles of diameter D_p,

$$\boxed{\eta\left(D_p\right) = 1 - \frac{c_{out}\left(D_p\right)}{c_{in}\left(D_p\right)} = 1 - \exp\left[-\frac{4}{\pi} \eta_f \frac{f_f}{1 - f_f} \frac{H}{D_f} \right]} \tag{9-59}$$

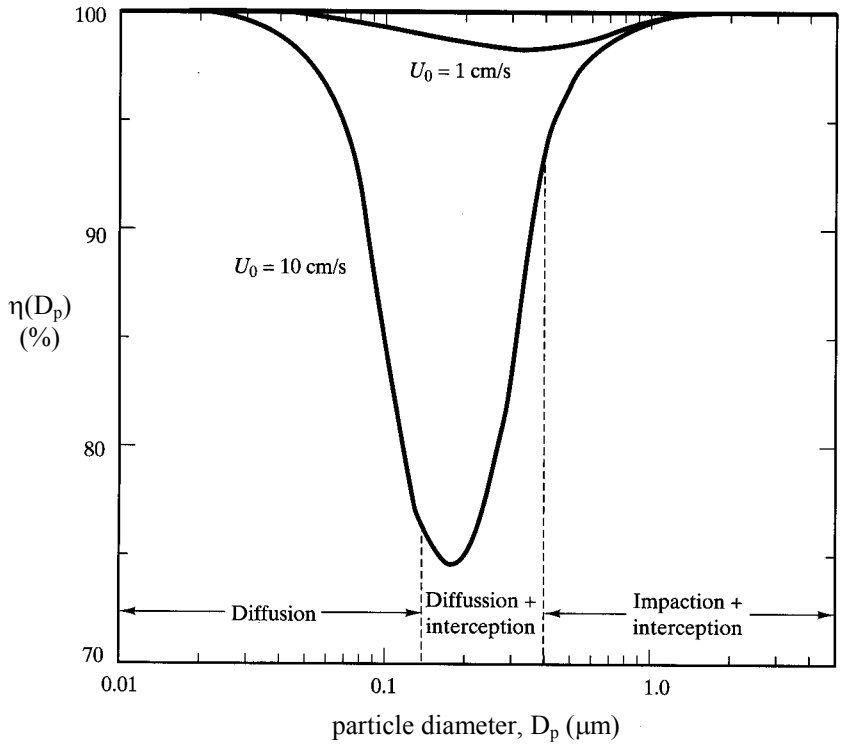

Figure 9.32 Filter grade efficiency for two face velocities; filter thickness H = 1.0 mm, solids fraction f_f = 0.05, single fiber diameter D_f = 2 μm (adapted from Hinds, 1982).

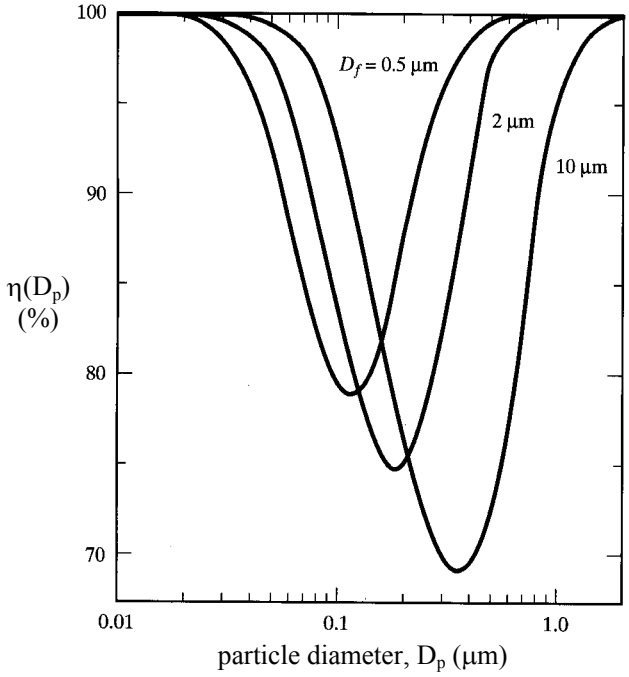

Figure 9.33 Filter grade efficiency for three fiber diameters (D_f); face velocity U_0 = 1.0 cm/s, solids fraction f_f = 0.05, filter thickness (H) adjusted to produce the same pressure drop for all three cases (adapted from Hinds, 1982).

9.5 Electrostatic Precipitators

Another method to clean unwanted aerosol particles from the air without using a scrubbing liquid is ***electrostatic precipitation***, which uses electrical charge to force particles to drift towards collecting plates, onto which the particles impact and are collected. Such a device is called an ***electrostatic precipitator*** (***ESP***).

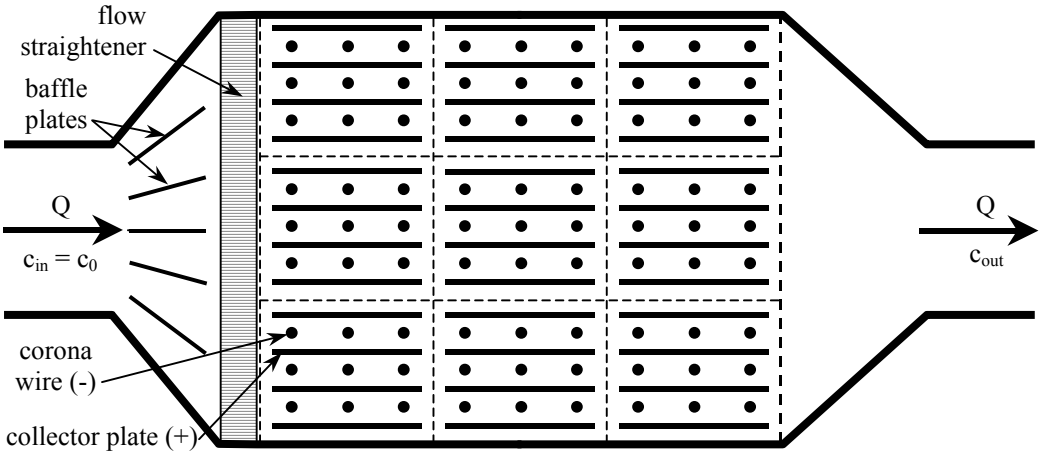

Figure 9.39 Top view of a negative ionization, single-stage, plate-wire ESP, with three parallel legs, each of which has three modules in series; circles represent the negatively charged corona wires, lines represent the positively charged collector plates.

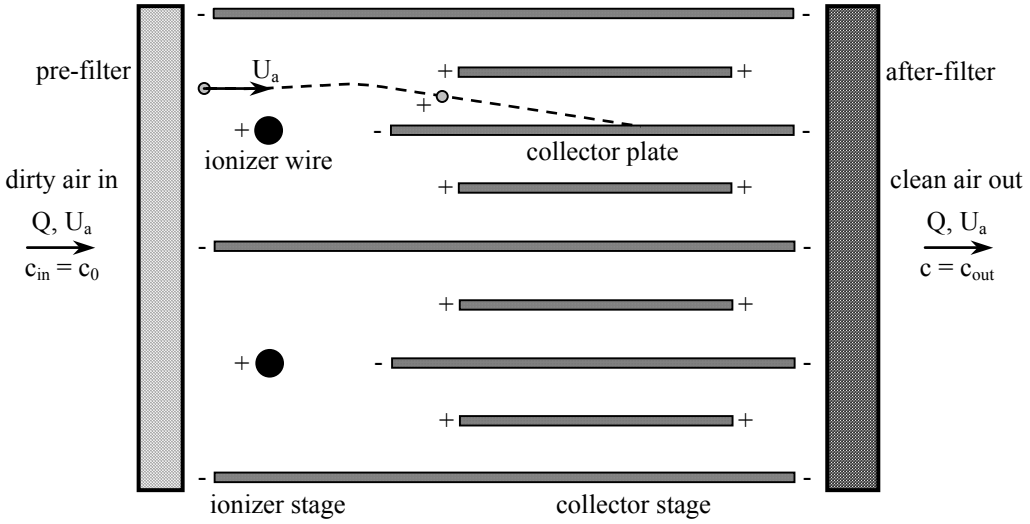

Figure 9.40 Schematic diagram of a positive ionization, two-stage, plate-wire ESP; dashed line indicates a particle trajectory.

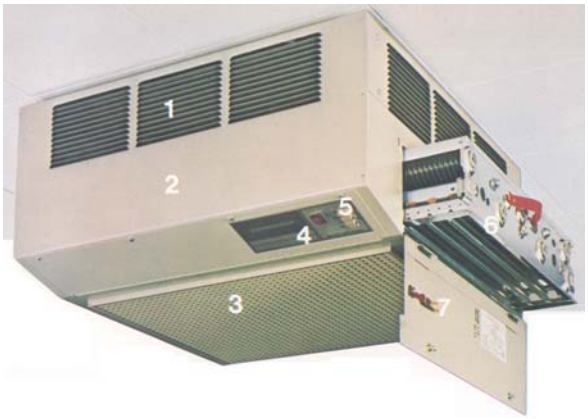

Figure 9.41 Smokemaster ceiling-mounted two-stage electrostatic precipitator that removes smoke, fume and small particles from public places; 1 – discharge louvers, 2 – housing, 3 – prefilters and grille, 4 – indicator lamp, 5 – speed control, 6 – ESP cells, 7 – access door (with permission of Air Quality Engineering).